Anaerobe 72 (2021) 102449

Contents lists available at ScienceDirect

Anaerobe

journal homepage: www.elsevier.com/locate/anaerobe

Original Article

Label-free quantitative proteomic analysis of the oral bacteria *Fusobacterium nucleatum* and *Porphyromonas gingivalis* to identify protein features relevant in biofilm formation

Marwan Mansoor Ali Mohammed [1, 3], Veronika Kuchařová Pettersen [*, 2, 3], Audun H. Nerland, Harald G. Wiker, Vidar Bakken

Department of Clinical Science, Faculty of Medicine, University of Bergen, Bergen, Norway

ARTICLE INFO

Article history:
Received 15 May 2021
Received in revised form
24 July 2021
Accepted 14 September 2021
Available online 17 September 2021

Handling Editor: Audrey N Schuetz

Keywords:
Bacterial biofilm
Planktonic bacteria
Riboflavin
Fusobacterium nucleatum
Porphyromonas gingivalis
Label-free quantitative proteomics

ABSTRACT

Background: The opportunistic pathogens *Fusobacterium nucleatum* and *Porphyromonas gingivalis* are Gram-negative bacteria associated with oral biofilm and periodontal disease. This study investigated interactions between *F. nucleatum* and *P. gingivalis* proteomes with the objective to identify proteins relevant in biofilm formation.

Methods: We applied liquid chromatography-tandem mass spectrometry to determine the expressed proteome of *F. nucleatum* and *P. gingivalis* cells grown in biofilm or planktonic culture, and as mono- and dual-species models. The detected proteins were classified into functional categories and their label-free quantitative (LFQ) intensities statistically compared.

Results: The proteomic analyses detected 1,322 *F. nucleatum* and 966 *P. gingivalis* proteins, including abundant virulence factors. Using univariate statistics, we identified significant changes between biofilm and planktonic culture (p-value $\leq$0.05) in 0,4% *F. nucleatum*, 7% *P. gingivalis*, and 14% of all proteins in the dual-species model. For both species, proteins involved in vitamin B2 (riboflavin) metabolism had significantly increased levels in biofilm. In both mono- and dual-species biofilms, *P. gingivalis* increased the production of proteins for translation, oxidation-reduction, and amino acid metabolism compared to planktonic cultures. However, when we compared LFQ intensities between mono- and dual-species, over 90% of the significantly changed *P. gingivalis* proteins had their levels reduced in biofilm and planktonic settings of the dual-species model.

Conclusions: The findings suggest that *P. gingivalis* reduces the production of multiple proteins because of the *F. nucleatum* presence. The results highlight the complex interactions of bacteria contributing to oral biofilms, which need to be considered in the design of prevention strategies.

1. Introduction

Fusobacterium nucleatum and *Porphyromonas gingivalis* are important colonizers of the subgingival biofilms [1]. Both bacteria play a role in the pathogenesis of periodontal diseases, a group of inflammatory diseases of the teeth supporting tissues [2]. A mild form called gingivitis is highly prevalent and can affect up to 90% of the worldwide population. However, gingivitis does not affect the underlying supporting structures of the teeth and is reversible. A more severe form of the disease, periodontitis, results in loss of connective tissue and bone support and is the main cause of tooth loss in adults [3].

F. nucleatum is a member of the Socransky's orange complex which comprises putative periodontal pathogens [1,4]. The bacterium is commonly cultivated from the subgingival biofilm and tends to aggregate with other oral bacteria, working as a bridge between early and late colonizers in the development of the dental biofilm [5]. A number of *F. nucleatum* virulence factors have been

* Corresponding author. UiT The Arctic University of Norway, Department of Medical Biology, Sykehusveien 44, 9019, Tromsø, Norway.
E-mail addresses: mmmohammed@sharjah.ac.ae (M.M. Ali Mohammed), veronika.k.pettersen@uit.no (V.K. Pettersen), audun.nerland@uib.no (A.H. Nerland), harald.wiker@uib.no (H.G. Wiker), vidar.bakken@uib.no (V. Bakken).
[1] Present Address: Department of Oral and Craniofacial Health Sciences, College of Dental Medicine, University of Sharjah, Sharjah, United Arab Emirates.
[2] Present Address: Department of Medical Biology, UiT The Arctic University of Norway, Tromsø, Norway.
[3] These authors contributed equally to this work.

https://doi.org/10.1016/j.anaerobe.2021.102449

characterized, including the heat-shock protein GroEL that activates host inflammatory factors [6], the outer membrane proteins Fap2 and RadD that are associated with adhesion and induction of host cells death [7], and other outer membrane adhesins such as FadA [6,8–11]. *P. gingivalis* is a member of the Socransky's red complex, a group of bacteria strongly associated with periodontal disease [12]. It is often found in the deep periodontal pockets, and it produces a broad array of potential virulence factors involved in tissue colonization and destruction as well as in perturbations of the host defence [13–15]. The most widely studied pathogenic factors produced by *P. gingivalis* are lipopolysaccharides, gingipains, and pili. These factors usually interact with Toll-like receptors during the progression of periodontitis [16].

P. gingivalis and *F. nucleatum* are considered strict anaerobes, and both species display a synergistic enhancement in biofilm formation and pathogenicity [17–19]. Several studies showed that the bacteria can grow in a partially oxygenated condition when grown together and suggested that enhanced production of oxidoreductive enzymes by *F. nucleatum* protects *P. gingivalis* from oxidative stress [20,21]. Similarly, *in vitro* and *in vivo* models showed a nearby association between the bacteria, indicating that they co-aggregate and potentially support each other in biofilm formation [18,22,23]. Other *in vitro* studies investigated *P. gingivalis* and/or *F. nucleatum* within a model oral microbial community and demonstrated changes in protein expression compared to single-species models, suggesting the importance of the interactions within the community [24–26]. However, how exactly *P. gingivalis* and *F. nucleatum* interact remains poorly understood.

Most microbiology research has been focused on free-floating bacteria in suspension (planktonic cells). However, recent investigations indicate that biofilm is the preferred form of life for most microbes, particularly those of pathogenic nature [27]. Further, mounting evidence indicates that cells growing in biofilms are in a very different physiological state [28–30]. For example, the envelope fraction of *Pseudomonas aeruginosa* cells grown as a biofilm showed a 30–40% difference in the detected proteins compared with the same fraction of *P. aeruginosa* cells grown in planktonic culture [28].

Previous proteomic studies showed how *P. gingivalis* interacts with other oral bacteria such as *Treponema denticola* [25] and *Streptococcus oralis* [31], as well as how its cell envelope proteome changes under biofilm growth condition when compared to the planktonic culture [32]. Further, whole-cell proteomics analyses of a three-species model community consisting of *P. gingivalis*, *F. nucleatum*, and *Streptococcus gordonii* described changes in energy metabolism [24] and that a community lifestyle provides physiological support for *P. gingivalis* [26]. We previously characterized biofilms of *F. nucleatum* and *P. gingivalis* when grown individually and together by confocal laser scanning microscopy, where we assessed their biomass and thickness [19], and by proteomics, where we characterized proteins within the extracellular matrix [33]. In the current study, we determined the differences between *P. gingivalis* and *F. nucleatum* cells grown in a culture and biofilm at the proteome level. To address how *F. nucleatum* and *P. gingivalis* interact in the two growth conditions, we grew the bacteria both individually and in dual-species model. The results showed that the two bacteria influence each other, and most markedly, *P. gingivalis* proteins displayed reduced levels of multiple proteins in the dual-species biofilm.

2. Materials and methods

2.1. Bacterial strains and growth conditions

Fusobacterium nucleatum subsp. *nucleatum* type strain ATCC 25586 and *Porphyromonas gingivalis* type strain ATCC 33277 were used in the current study. Anaerobic conditions (5% CO_2, 10% H_2, and 85% N_2) (Anoxomat System, MART Microbiology, Lichtenvoorde, The Netherlands) were used in all steps of the experiment. For the biofilms preparations, the bacterial strains were grown first on fastidious anaerobic agar (FAA) plates at 37 °C for 48 h. Few colonies were then taken to inoculate Brucella broth cultures (Becton Dickinson, Maryland, USA) supplemented with 5 μg/ml hemin and 0.25 μg/ml Vitamin K. The bacteria were grown overnight in the liquid medium at 37 °C. The overnight cultures of *F. nucleatum* and *P. gingivalis* were adjusted to an absorbance of 0.15 at 600 nm (A_{600}), of which 10 ml (5 ml from each species in dual-species biofilm) was transferred to a separate 25 cm^2 (area) polystyrene cell culture flasks (TPP Techno Plastic Products, Trasadingen, Switzerland). The absorbance of 0.15 measured at 600 nm corresponded to approximately 2-3 x 10^7 and 1-2 x 10^8 CFU per ml for *F. nucleatum* and *P. gingivalis*, respectively. Because both *F. nucleatum* and *P. gingivalis* are slow-growing bacteria, we incubated the flasks at 37 °C for 4 days, using a previously published protocol [33]. The medium was then removed, and the biofilm samples were washed once with phosphate buffered saline (PBS) before the biofilms were harvested with a cell scraper (Nunc, Rochester, NY, USA). The biofilm samples were resuspended in 500 μl PBS and stored at −20 °C until further processing.

The planktonic cultures were anaerobically grown in the same liquid medium described above in 10 ml glass round bottom test tubes with screw caps at 37 °C, without shaking. After 4 days, free-floating bacteria were collected by centrifugation at 3000×*g* for 3 min at room temperature. The pelleted cells were resuspended in 500 μl PBS and stored at −20 °C until further processing. The viability of the bacterial cells was determined by CFU counting of the initial inoculum and of the mature cultures/biofilms in 3 independent biological replicates as previously described [33].

2.2. Protein extraction from the biofilm and planktonic samples

The harvested cells were processed according to a standard protocol for bacterial cells [34]. Briefly, the cells were washed 3 times by resuspension in 1 ml PBS and centrifugation for 10 min each time at 6000×*g* at +4 °C. In a final step, the cells were resuspended in 1 ml of extraction buffer (10 mM Tris-HCl, 2.5% SDS, pH 8.0). The cell suspensions were transferred to FastPrep® Lysing Matrix A, 2 mL Tube (MP Biomedicals, California, USA) and then bead-beated in FastPrep® FP120 Cell Homogenizer (Thermo, California, USA) for 45 s at 6.5 m/s. The cell extracts were cooled on ice for 5 min, then the cell debris was removed by 30 min centrifugation at 10,000×*g*, +4 °C. The collected supernatant was kept on ice until measurements of protein concentrations using Direct Detect® Spectrometer (Merck Millipore, Darmstadt, Germany). No protease inhibitors were added to the protein extraction buffer because of previously reported interference with trypsin digestion [35], leading to fewer detected proteins. Subsequent sample treatment, including protein solubilization and denaturation, further eliminated the need for protease inhibitors.

2.3. Sample preparation for the proteomic analysis

Protein extracts from the biofilm and planktonic cells prepared from 3 independent biological replicates were subjected to the Filter Aided Sample Preparation method [36]. This approach based on spin filters eliminates the need for proteinase inhibitors because the hoarse conditions created by 8M urea buffer suppress any potential proteolytic activity. The protein samples were mixed with a solution of 10 mM dithiothreitol (DTT) in 100 mM ammonium bicarbonate (NH_4HCO_3) [solution to total protein ratio (v/w) 1:10]

and incubated for 45 min at 56 °C. The Microcon device YM-10 filters (Molecular weight cut-off 10kDA, Merck Millipore, Darmstadt, Germany) were first conditioned by adding 100 μl of urea buffer (8 M urea, 10 mM HEPES, pH 8.0) and centrifuged at 14,000×*g* for 5 min. Aliquots of the samples containing 50 μg of protein were mixed with 200 μl urea buffer in the filter unit and centrifuged at 14,000×*g* for 15 min, and this step was repeated. The filtrate was discarded, and 100 μl of 0.05 M iodoacetamide was added to each sample. The samples were mixed at 600 rpm for 1 min and incubated without mixing in the dark for 20 min, followed by centrifugation at 14,000×*g* for 10 min, 3 washes with 100 μl urea buffer, and 3 washes with 100 μl 40 mM NH_4HCO_3. Proteins retained on the filter were digested with trypsin (Thermo Fisher Scientific, IL, USA) in 40 mM NH_4HCO_3 buffer (enzyme to protein ratio 1:50) at 37 °C for 16 h. The released peptides were collected by adding 50 μl of MS grade water followed by centrifugation at 14,000×*g* for 15 min. This step was repeated twice. The samples were concentrated in a vacuum concentrator (Eppendorf, Hamburg, Germany).

2.4. Filtration and desalting

StageTips to be used for filtration and peptide samples desalting were prepared in-house according to the protocol developed by Rappsilber and colleagues [37]. Shortly, 3M Empore C18 extraction disks (3M, Minnesota, USA) were packed in 200 μl pipet tips by a blunt-ended needle and a plunger or metal rod that helped fit the extracted disks in the pipet tips. The disks were then wetted by passing 20 μl of methanol, followed by 20 μl of elution buffer [80% acetonitrile (ACN), 0.1% formic acid (FA)]. The disks were conditioned and equilibrated with 20 μl of 0.1% FA just before the last residue of the previous buffer left the tip to avoid drying of the disks. The prepared peptide mixtures (volumes 20–40 μl) were loaded on top of the Stage Tip. The peptide samples were first desalted by washing with 20 μl of 0.1% FA and then eluted by adding 20 μl of the elution buffer two times. The collected samples were dried in the vacuum concentrator and stored at −80 °C until further analyses. Peptide samples were resuspended by adding 1 μl of 100% FA and 19 μl of 2% ACN prior to liquid chromatography-tandem mass spectrometry (LC-MS/MS) analysis.

2.5. LC-MS/MS

The MS/MS analysis was carried out at the Proteomics Unit, University of Bergen (PROBE), on an Ultimate 3000 RSLC system (Thermo Scientific) connected to a linear quadrupole ion trap-Orbitrap (LTQ-Orbitrap) MS (Thermo Scientific) equipped with a nanoelectrospray ion source. Briefly, 1 μg protein was loaded onto a pre-concentration column (Acclaim PepMap 100, 2 cm × 75 μm i.d. nanoViper column, packed with 3 μm C18 beads) at a flow rate of 5 μl/min for 5 min using an isocratic flow of 0.1% trifluoroacetic acid, vol/vol (TFA). Peptides were separated during a biphasic ACN gradient from two nanoflow ultra-performance liquid chromatography (UPLC) pumps (flow rate of 270 nl/min) on the analytical column (Acclaim PepMap 100, 50 cm × 75 μm i.d. nanoViper column, packed with 3 μm C18 beads). Solvent A and B were 0.1% FA (vol/vol) in water or ACN (vol/vol), respectively. Separated peptides were sprayed directly into the MS instrument during a 195 min LC run with the following gradient composition: 0–5 min 5% B, 5–6 min 8% B, 6–135 min 7–32% B, 135–145 min 33–40% B, and 145–150 min 40–90% B. Elution of very hydrophobic peptides and conditioning of the column was performed by isocratic elution with 90% B (150–170 min) and 5% B (175–195 min), respectively. Desolvation and charge production were accomplished by a nanospray Flex ion source.

The mass spectrometer was operated in the data-dependent-acquisition mode to automatically switch between Orbitrap-MS and LTQ-MS/MS acquisition. Survey of full-scan MS spectra (from m/z 300 to 2,000) were acquired in the Orbitrap with a resolution of R = 240,000 at m/z 400 (after accumulation to a target of 1,000,000 charges in the LTQ). The method used allowed sequential isolation of the most intense ions (up to 10, depending on signal intensity) for fragmentation on the linear ion trap using collision-induced dissociation at a target value of 10,000 charges. Target ions already selected for MS/MS were dynamically excluded for 18s. General mass spectrometry conditions were as follows: electrospray voltage, 1.8 kV; no sheath; and auxiliary gas flow. Ion selection threshold was 1,000 counts for MS/MS, and an activation Q-value of 0.25 and activation time of 10 ms was also applied for MS/MS.

2.6. Data analysis

The acquired MS raw data were processed by using the MaxQuant software [38], version 1.5.2.8, with default settings and the following additional options: Label-Free Quantification (LFQ), match between runs, and 0.01 false discovery rate (FDR) at both peptide and protein level. Data analysis was carried out by analysing each species separately, similarly as previously described [39]; single-species files were analysed together with the dual-species files and the protein database of the specific species. Specifically, the MS spectra were searched against matching protein databases for the strains used in this study (*F. nucleatum* type strain ATCC 25586 and *P. gingivalis* type strain ATCC 33277), downloaded from the Universal Protein Knowledgebase (UniProtKB) on the 4th of February 2015. Using strain-specific databases allowed for accurate assignment of the proteins, and we did not detected any cross identification between *F. nucleatum* and *P. gingivalis* proteins. Normalized spectral protein intensities (LFQ intensity) were derived by the MaxLFQ algorithm. To make comparable the mono- and dual-species samples, which have different ratios of the species, MaxLFQ applies correction coefficients during the normalisation process [40].

MaxQuant output data were analysed with the Perseus module [41]. The post MaxQuant analysis included filtering the generated 'proteingroups.txt' table for contaminants, only identified by site and reverse hits. Each protein identified in at least 2 of the 3 replicates was considered valid. Proteins with significant differential levels were identified by statistical analysis based on two-sided *t*-test, which was performed on proteins $\log_2$ transformed LFQ values. A protein was considered significantly changed if it was marked as significant in the *t*-test and showed more than 2 $\log_2$ difference from the mean LFQ intensity.

Functional protein classification was performed by using The Database for Annotation, Visualization and Integrated Discovery (DAVID) [42] and QuickGO annotation database [43]. The gene names, including ordered locus, were downloaded from UniProtKB, using the Retrieve/ID mapping function and UniProt protein identifiers. Potentially interesting clusters identified by DAVID were studied individually. The web-based application SOSUI-GramN [44] was used to predict the subcellular localization of the identified proteins. The mass spectrometry proteomics data have been deposited to the ProteomeXchange Consortium via the PRIDE partner repository with the dataset identifier PXD008288 [45]. Fig. 4 was created using diagrams from BioRender.com.

3. Results

This study's objective was to investigate proteins relevant for biofilm formation. We grew the bacteria in mono- or dual-species

models and either as biofilms or planktonic cells. Altogether, six different growth conditions (biofilms and planktonic cultures of *F. nucleatum*, *P. gingivalis,* and the dual-species model) were analysed by LC-MS/MS using 3 biological replicates for each condition.

3.1. LFQ proteomic analysis of F. nucleatum and P. gingivalis grown in biofilm or planktonic culture and individually or together

The analysis yielded approximately a million MS/MS spectra, which we searched against strain-specific protein databases of either *F. nucleatum* or *P. gingivalis*. The data search matched the spectra to 23,423 distinct peptide sequences (Table S1, Supplementary file 1), which were assigned to 2,288 different proteins (Table S2, Supplementary file 1). The number of identified proteins in each growth condition and their predicted subcellular localization are shown in Table 1.

The proteome coverage, which we defined as the number of the detected proteins divided by the theoretical proteome derived from the UniProt database, was ≈ 62% for *F. nucleatum* and ≈ 43% for *P.* gingivalis in both biofilm and planktonic conditions in the mono-species models (Table 1). Up to 84% of all identified proteins (1,916) were described by LFQ intensities, which indicate relative protein levels in the analysed samples (Table S3, Supplementary file 1). The LFQ intensities covered a dynamic range of ≈ 12 $\log_2$ (Fig. S1, Supplementary file 2), and the correlations between replicates, represented as the Pearson correlation coefficient, varied between 0.79 and 0.98 (Fig. S2, Supplementary file 2).

3.2. F. nucleatum and P. gingivalis virulence factors are among the most abundant proteins produced under in vitro conditions

The most abundant proteins identified in the biofilm and planktonic lifestyles (Table 2) included oxidoreductases, acyltransferases, outer membrane proteins, and proteases, among others. We identified major virulence factors of *F. nucleatum* and *P. gingivalis* (*e.g.*, major outer membrane protein FomA and Lys-gingipain) as well as cytoplasmic proteins like Acetyl-CoA acetyltransferase, Alkyl hydroperoxide reductase C22 protein, and Neutrophil-activating protein A, which were previously shown to be abundant in the biofilms extracellular polymeric matrix [33]. The latter finding confirms that proteins released from dead cells are used in the biofilm matrix [46].

Five of 10 most abundant *F. nucleatum* and *P. gingivalis* proteins detected in the planktonic culture were also identified as the most abundant in the biofilm (Table 2). Yet, none of these proteins were among significantly changed proteins (see below) between the planktonic and biofilm conditions. Identification of the same proteins in both culturing conditions is likely a result of using the same medium and the same length of time for both planktonic culture and biofilm. *F. nucleatum* glutamate dehydrogenase (FN0488) is an example of such an abundant protein; this protein is involved in the oxidation-reduction process and can be used as a diagnostic marker for the genus *Fusobacterium* [47].

Other *F. nucleatum* proteins detected at high levels were oxidoreductases, outer membrane proteins, and adhesins. Examples of these are FN1526 (known as RadD), which is an arginine-inhibitable adhesin required for inter-species adherence, and FN1859 (known as FomA), which functions as a non-specific porin and a virulence factor facilitating bacterial evasion from host immune surveillance [48]. *P. gingivalis* proteins detected at high levels in planktonic culture and biofilm included virulence-related proteases cysteine proteinase RgpA and Lys-gingipain (Kgp). These proteins are involved in the subversion of leukocytes and microbial dysbiosis, facilitating *P. gingivalis* colonization and the outgrowth of the surrounding microbial community [49].

To identify proteins produced in differential amounts by cells either in the biofilm or planktonic culture, we statistically compared LFQ intensities by the student *t-test* ($p \leq 0.05$). Similarly, we compared the LFQ intensities of proteins produced by cells grown under either mono- or dual-species conditions (Table S4, Supplementary file 2).

3.3. F. nucleatum proteome is relatively similar under biofilm and planktonic conditions

Five out of 1,070 *F. nucleatum* proteins, which were quantified under both biofilm and planktonic culture, showed a significant change in their LFQ levels (Fig. 1A). Proteins with significantly increased levels in the biofilm (Table S5) were Thiazole synthase (ThiC) and phosphomethylpyrimidine synthase (ThiG) involved in vitamin B1 (thiamine) and vitamin B2 (riboflavin) metabolic processes. *F. nucleatum* proteins with increased LFQ levels in the planktonic condition were a membrane transport protein (IIC component protein of the PTS system) and two transferases (Acetate CoA-transferase YdiF and Acetoacetate: butyrate/acetate coenzyme A transferase).

Some of the proteins associated with *F. nucleatum* pathogenicity were identified as significantly different ($p \leq 0.05$) but showed less than 2 $\log_2$ difference between the biofilm and planktonic cultures (Table S5). For example, metal-dependent hydrolase (FN1210), a resistance-causing and drug efflux protein with beta-lactamase activity [9] had slightly increased LFQ levels in the biofilm mode of growth. Three other proteins (FN1613, FN0268, FN0235), which are virulence factors with peptidase activity and are involved in proteolysis, also had increased levels in the biofilm.

Table 1
The number of identified proteins in each condition categorized according to predicted cellular localization.

Subcellular localization[a]	Biofilm			Planktonic culture		
	FnBio	PgBio	FnPgBio[c]	FnPla	PgPla	FnPgPla[c]
Cytoplasmic	893	552	683 + 315	904	483	868 + 264
Extracellular	45	27	34 + 22	44	28	43 + 19
Inner membrane	210	131	144 + 72	216	125	198 + 69
Outer membrane	34	92	30 + 65	36	88	35 + 72
Periplasm	21	73	18 + 51	20	72	17 + 55
Unknown	54	42	39 + 19	54	38	55 + 23
Total Detected	1257	917	948 + 544	1274	834	1216 + 502
Proteome coverage[b] (%)	61.3	45.3	46.3 and 26.9	62.2	41.2	59.3 and 24.8

Abbreviations: Fn = *F. nucleatum*, Pg = *P. gingivalis*, Bio = Biofilm, Pla = Planktonic.
[a] The predictions were made by using the web-based application SOSUI-GramN [44].
[b] The number of detected proteins divided by the theoretical proteome (Fn 2049 proteins, Pg 2022 proteins) derived from the UniProt database.
[c] Numbers of detected Fn and Pg proteins, respectively.

Table 2
Top abundant *F. nucleatum* and *P. gingivalis* proteins identified in different culturing conditions.

Gene	Protein Description	Major Function	Mono-species model[a] (log_2 LFQ)		Dual-species model[a] (log_2 LFQ)	
F. nucleatum			Biofilm	Planktonic	Biofilm	Planktonic
FN0488	Glutamate dehydrogenase	oxidoreductase	**32.66**	**31.26**	30.04	**31.66**
FN1024	DNA-binding protein HU	DNA binding protein	**32.08**			
FN1535	Acyl-CoA dehydrogenase, short-chain specific	oxidoreductase	**32.02**	**31.29**	28.89	31.19
FN1983	Alkyl hydroperoxide reductase C22 protein	oxidoreductase	**31.90**	30.37	**30.99**	30.12
FN1170	Pyruvate-flavodoxin oxidoreductase	oxidoreductase	**31.79**	**31.77**	29.93	**31.53**
FN1165	D-galactose-binding protein	metal ion binding protein	**31.72**	**32.07**	30.34	**31.61**
FN1943	Tryptophanase	lyase	**31.57**	30.71	29.88	31.32
FN1526	Fusobacterium outer membrane protein family	OMP/adhesin	**31.43**	**31.74**	30.39	**31.83**
FN1859	Major outer membrane protein FomA	OMP/VF	**31.29**	30.71	**31.02**	**32.39**
FN0495	Acetyl-CoA acetyltransferase	acetyltransferase	**31.28**	30.20	**32.11**	30.27
FN0396	Dipeptide-binding protein	peptide transporter	31.10	**32.37**	**30.88**	**31.50**
FN1911	Outer membrane protein	OMP	30.61	**31.44**	26.16	30.53
FN1079	Neutrophil-activating protein A	ferric iron binding protein	30.78	**31.42**	30.59	30.99
FN0262	Formate acetyltransferase	acetyltransferase	30.15	**31.25**	30.11	31.20
FN1549	Stomatin like protein	—	29.95	**31.13**	29.46	30.29
FN1019	3-hydroxybutyryl-CoA dehydrogenase	oxidoreductase	30.59	30.16	**31.74**	30.35
hutH1	Histidine ammonia-lyase 1	lyase	28.93	27.69	**31.12**	28.26
P. gingivalis			Biofilm	Planktonic	Biofilm	Planktonic
rgpA	Arginine-specific cysteine proteinase RgpA	protease/VF	**32.04**	**32.93**	**32.75**	**31.91**
rplL	50S ribosomal protein L7/L12	ribosomal protein	**31.17**	27.32	28.42	23.58
kgp	Lys-gingipain	protease/VF	**31.04**	**32.28**	**32.59**	31.19
gdh	NAD-specific glutamate dehydrogenase	oxidoreductase	**31.03**	27.65	29.83	26.24
hagA	Hemagglutinin protein HagA	erythrocyte agglutinating protein/VF	**30.85**	**32.66**	**31.47**	**31.74**
ragA	Receptor antigen A	protein with receptor activity	**30.66**	**33.52**	**31.30**	**33.14**
ragB	Receptor antigen B	protein with receptor activity	**30.52**	**32.97**	28.93	**32.92**
PGN_0235	DNA-binding protein HU	DNA binding protein	**30.52**	28.39	27.54	25.49
PGN_0727	4-hydroxybutyryl-CoA dehydratase	oxidoreductase	**30.03**	30.75	30.55	25.38
PGN_0659	35 kDa hemin binding protein	hemin binding protein/VF	**29.44**	**30.02**	29.15	28.83
PGN_0727	4-hydroxybutyryl-CoA dehydratase	oxidoreductase	30.03	**30.75**	30.55	25.38
PGN_0898	Probable peptidylarginine deiminase	deiminase/VF	30.24	**30.49**	29.41	28.32
PGN_0729	Outer membrane protein 41	OMP/immunoreactive protein	29.08	**30.37**	28.45	29.78
gdh	NAD-specific glutamate dehydrogenase	oxidoreductase	31.03	**29.83**	27.65	26.33

[a] Median of proteins log_2 LFQ intensities across 3 replicates. The most abundant proteins for each condition are shown in bold. Abbreviations: OMP = outer membrane protein, VF = virulence factor.

3.4. *P. gingivalis* increases the production of some proteins when cultured in biofilm compared to the planktonic condition

Approximately 7% of all *P. gingivalis* proteins quantified under biofilm and planktonic culture (40 out of 593) showed significant changes in their LFQ levels (Table S6). We detected 30 proteins with more than $2log_2$ LFQ levels increase in the biofilm setting (Fig. 1B). As in *F. nucleatum* biofilm, riboflavin biosynthesis protein (RibBA) had increased levels in the *P. gingivalis* biofilm. The latter coincides with a transcriptomic study, which showed that the protein is upregulated in a *P. gingivalis* biofilm [50]. This protein is involved in biofilm-related functions, including quorum sensing signalling and extracellular electron transfer in different bacterial species [51,52]. Other proteins that increased in the biofilm were functional in translation (RplK, RplL, RplP, RpsA) and amino acid biosynthesis (GpmA, PGN_0692).

We identified 10 *P. gingivalis* proteins with increased amounts in the planktonic condition, including outer membrane efflux protein (PGN_1432) that has cellular transport activity, an integral component of membrane (PGN_0296), immunoreactive 23 kDa antigen protein (PGN_0482), and membrane-associated zinc metalloprotease (PGN_1582) that has peptidase activity and is involved in proteolysis.

Overall, these results support findings from a gene expression analysis study, which showed that *P. gingivalis* genes are upregulated in the biofilm setting compared to planktonic culture [50].

Both F. nucleatum and P. gingivalis detected proteomes display changes between biofilm and planktonic culture when co-cultivated as dual-species model.

In the dual-species cultures, 797 proteins were quantified under both biofilm and planktonic conditions, and LFQ intensities of 14% (112) proteins were significantly changed (Fig. 1C). Among these, we detected more proteins derived from *F. nucleatum* (72) than *P. gingivalis* [40]. Of 78 proteins with increased amounts in the biofilm (Table S7), 41 derived from *F. nucleatum* and included the following functional clusters: lyase (9 proteins), metal binding (8 proteins), and energy production and conversion (4 proteins). The remaining 37 proteins were derived from *P. gingivalis* (Fig. 1D) and included proteins with oxidoreductase (4 proteins) and translation (4 proteins) activity.

Most of the proteins with increased levels in the dual-species planktonic culture were derived from *F. nucleatum* (31 out of 34) and included 7 ribosomal proteins, 4 proteins involved in rRNA binding, and 6 translational proteins.

3.5. *F. nucleatum* marginally changes its proteome in response to *P. gingivalis* presence

Eleven out of 635 *F. nucleatum* proteins that were quantified both in the mono- and dual-species biofilm showed significantly different levels (Fig. 2A and Table S8). The three proteins with increased levels in the dual-species biofilm were an uncharacterized membrane protein (FN0514), transcriptional regulatory protein (FN0198), and multi-functional protein HppA that is involved in potassium ion transport. Proteins with increased levels in the mono-species biofilm included outer membrane proteins

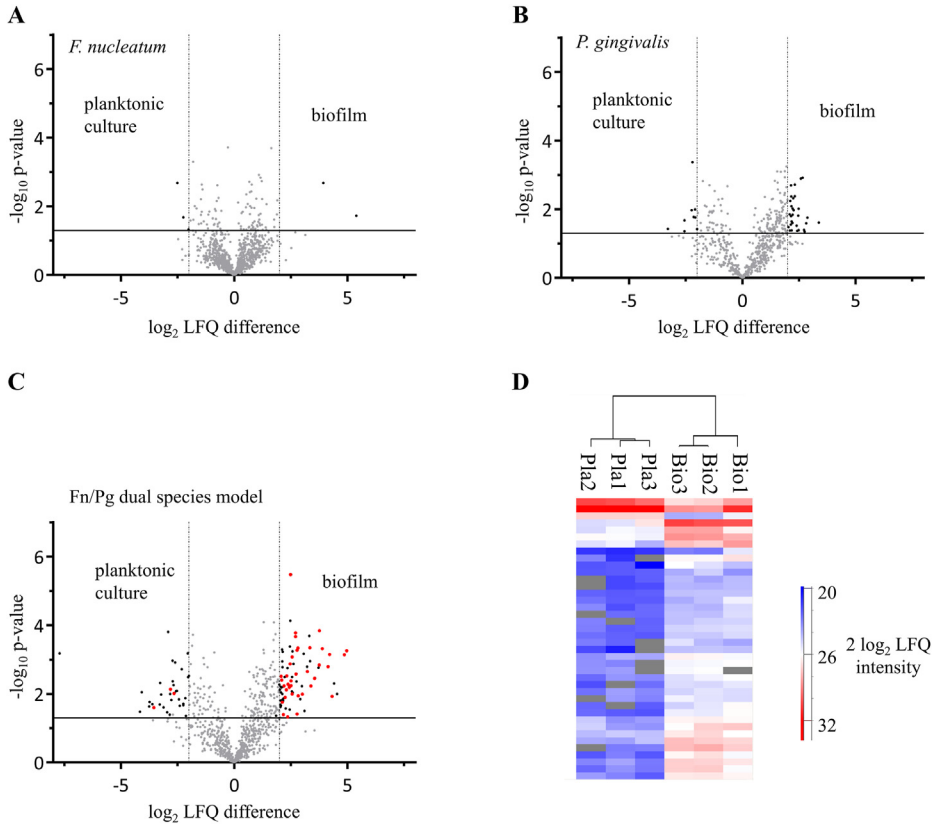

Fig. 1. Differentially produced proteins in the biofilm and planktonic modes of growth. Volcano plots show results of *t*-test (p-value ≤0.05), which was performed on $\log_2$ LFQ intensities of proteins derived either from biofilm or planktonic cells of **A)** *F. nucleatum* (1069 proteins), **B)** *P. gingivalis* (593 proteins), and **C)** dual-species model (797 proteins). The *t*-test identified 5, 40, and 112 proteins as having significantly different levels (≥2 $\log_2$ LFQ intensity) between the two conditions in A, B, and C, respectively (shown in black). The horizontal line shows the p-value cut-off of 0.05, and the vertical lines mark the $\log_2$ LFQ intensity = ±2. Red dots in C denote *P. gingivalis* proteins. **D)** Hierarchical clustering of 40 *P. gingivalis* proteins with significantly different $\log_2$ LFQ intensities in the dual-species model. Abbreviations: Pla – planktonic culture, Bio – biofilm. Biological replicates are shown, and grey fields indicate missing values, *i.e.*, the protein was not detected, or its amounts were below quantifiable levels. (For interpretation of the references to color in this figure legend, the reader is referred to the Web version of this article.)

(FN0335, FN2103, and FN1449) and several uncharacterized proteins.

In the planktonic conditions, 10 out of 998 proteins showed significant changes. Two proteins had increased levels in the dual-species model, while 8 decreased in the mono-species culture (Fig. 2B and Table S9). Most of these proteins were annotated as uncharacterized. Thus, the results suggest that *F. nucleatum* responds to the presence of *P. gingivalis* only mildly, mostly by decreasing production of specific proteins.

3.6. *P. gingivalis* reduces its protein production in biofilm in response to *F. nucleatum* presence

We identified 283 *P. gingivalis* proteins that were quantified both in the mono- and dual-species biofilms and most of the proteins with significantly different levels were decreased in the dual-species biofilm (51 out of 56) (Fig. 2C and Table S10). Functional analysis of these proteins pointed out the following functional clusters: structural ribosomal activity (6 proteins), translation (6 proteins), oxidation-reduction (4 proteins), and RNA binding (4 proteins).

Statistical comparison of *P. gingivalis* proteins LFQ intensities between the mono-species and dual-species planktonic cultures identified 63 significantly different proteins, and 59 of these showed reduced levels in the dual-species culture (Fig. 2D and Table S11). Twenty-six of the proteins with decreased levels in dual-species planktonic culture were also decreased in the dual-species biofilm condition (Table S10). In summary, when *P. gingivalis* cells were grown in the dual-species model, we detected a relatively high number of proteins that had reduced levels both in biofilm and planktonic culture.

4. Discussion

This study has explored the expressed proteomes of two important oral pathogens and showed how different growth conditions affect their proteins' qualitative and quantitative composition. We previously showed that *P. gingivalis* and *F. nucleatum* can form biofilm on both glass and polystyrene surfaces [19,33], and for practical reasons, we used polystyrene flasks to grow the biofilms, while planktonic cultures were cultivated in glass flasks. Whether and how the different surfaces affect the bacteria protein expression is currently unknown. Although some of the observed protein changes might be related to the surface used to grow the bacteria, we predict that the interactions between *P. gingivalis* and *F. nucleatum* cells have a stronger effect than those between the bacteria and the abiotic surfaces.

F. nucleatum proteins dominated the dual-species model under the experimental conditions used (Table 1). Still, the bioinformatics analysis predicted a higher number of detected outer membrane and periplasmic proteins for *P. gingivalis*. However, we suspect that some of the *F. nucleatum* proteins with unknown function might fall into the category of outer membrane and periplasmic proteins. The overall numbers of detected proteins were similar to previous

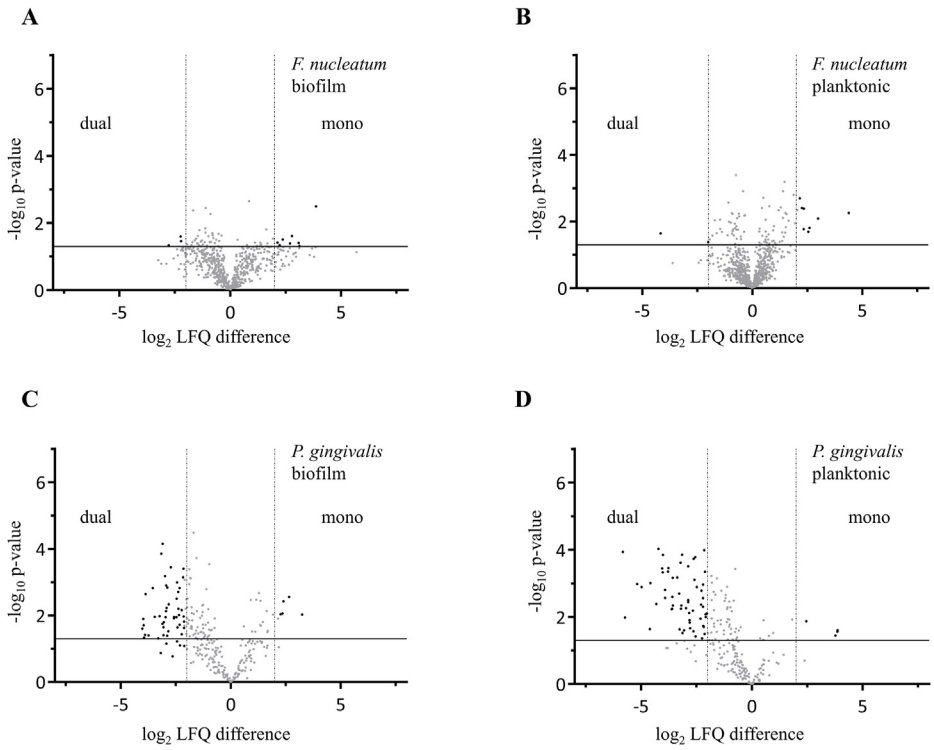

Fig. 2. Differentially expressed proteins in mono- and dual-species biofilms and planktonic growth conditions. Volcano plot shows results of *t*-test with p-value ≤0.05, which was performed on $\log_2$ LFQ intensities for **A)** *F. nucleatum* biofilm vs. dual-species biofilm (635 proteins), **B)** *F. nucleatum* planktonic vs. dual-species planktonic cultures (998 proteins), **C)** *P. gingivalis* biofilm vs. dual-species biofilm (283 proteins), **D)** *P. gingivalis* planktonic vs. dual-species planktonic cultures (242 proteins). The *t*-test identified 11, 10, 56, and 63 proteins as having significantly different levels (≥2 $\log_2$ LFQ intensity) between the two conditions in A, B, C, and D, respectively (shown in black). The horizontal line shows the p-value cut-off of 0.05, and the vertical lines mark the $\log_2$ LFQ intensity = ±2.

studies that reported proteome coverage between 48 and 60% for *P. gingivalis* [26,53] and 58% for *F. nucleatum* [24]. Growing the bacteria both individually and together allowed us to analyse interactions between the two species. Similarly, comparing the bacterial proteomes produced by cells harvested from planktonic cultures and biofilms highlighted proteins contributing to the specific growth conditions.

We observed relatively few differences in the *F. nucleatum* proteome between biofilm and planktonic conditions; however, other researchers have described more differentially produced proteins [30]. This is because we have applied a stricter cut-off, considering only statistical significance for proteins with ($p \leq 0.05$) and larger than 2 $\log_2$ difference in the LFQ intensities between conditions. If we apply ($p \leq 0.05$) with 1.5 $\log_2$ cut-off, we get 45 proteins (25 increase and 20 decreased) in the biofilm condition (Table S5), which is near to a recently published number (51 with 20 decreased and 31 increased) using the 2D gel method and a 1.5-fold difference [30].

Among *F. nucleatum* proteins with significantly increased levels in the biofilm (Table S5) were ThiC and ThiG proteins involved in vitamin B1and B2 metabolic processes. It is currently unknown if vitamin B1 or B2 are aiding *F. nucleatum* biofilm formation. However, cells of the anaerobic Gram-negative bacterium *Thermotoga maritima* that were grown as a biofilm exhibited increased transcription of genes involved in the biosynthesis of thiamine [54]. Although beyond the scope of the current study, it would be interesting to investigate the role of vitamin B1 and B2 metabolic processes in biofilm formation. Using a functional genomics approach, the *thiG* and *thiC* genes could be deleted from the *F. nucleatum* genome, and the phenotype of the resulting knockout strains in mono- and dual-species biofilm, as well as planktonic culture, characterised. In a similar fashion could be assessed the impact of deleting the gene for *P. gingivalis* riboflavin biosynthesis protein (RibBA) on mono- and dual-species biofilm as well as in planktonic growth.

In the dual-species biofilm, the FadA adhesion proteins (FN0249 and FN0264) displayed almost 8-fold and 4-fold reduction, respectively, compared to the planktonic culture (Table S7), while showed no change in the mono-species models (Table S5). FadA helps *F. nucleatum* to adhere and invade host epithelial and endothelial cells [55]. It also promotes colorectal carcinogenesis in humans by modulating signalling of E-cadherin/b-catenin, which was identified as the endothelial receptor for FadA [8]. The reduction in FadA levels might be explained by a recent study, which showed that *P. gingivalis* could suppress an invasion of *F. nucleatum* into gingival epithelial cells [56]. The authors attributed this to the degradation of E-cadherin by *P. gingivalis* gingipains [57]. Our results confirm that the presence of *P. gingivalis* has a negative effect on *F. nucleatum* FadA proteins.

While *F. nucleatum* proteome remained relatively similar under biofilm and planktonic conditions, *P. gingivalis* increased the production of many proteins when cultured in biofilm. The latter finding might reflect an adaptation of *P. gingivalis* to the biofilm condition. In biofilm, *P. gingivalis* appeared to generally increase the production of proteins functional in translation, oxidation-reduction, and biosynthesis of riboflavin and amino acids. The identification and quantification of these proteins provide new insights into the biology of this periodontal pathogen, adding additional information to previous gene expression studies [50,58]. These studies observed differential expression of *P. gingivalis* genes involved in functions related to the oxidative stress, cell envelope, transposons and metabolism, when compared biofilm growth

condition with planktonic culture. Although studies using microarray technology provide important information, not all transcripts might be translated to proteins. Moreover, protein abundance is a combined result of protein synthesis and degradation, the latter being ignored in transcriptomic studies.

Four out of 10 *P. gingivalis* proteins with increased levels in the planktonic condition were identified as outer membrane proteins. A compiled outer membrane proteome of *P. gingivalis* was recently published, including the predicted function of the identified proteins PGN_1432, PGN_0296, and PGN_0482 [59]. In addition, earlier studies showed that the outer membrane efflux protein PGN_1432 is a target of the HaeR regulator that modulates the acquisition and transport of heme [60], and the PGN_0482 immunoreactive protein has been linked to an inflammatory response in primary periodontal ligament fibroblasts [61].

The presence of *P. gingivalis* had a moderate impact on the *F. nucleatum* expressed proteome (Fig. 3A), significantly affecting 1–2% of the quantified proteins (Table S4). On the other hand, the change in *P. gingivalis* protein expression was much more pronounced (Fig. 3B). We detected alterations in the amounts of 19–26% *P. gingivalis* proteins when co-culture with *F. nucleatum* (Table S4). Moreover, over 90% of the significantly changed *P. gingivalis* proteins had their levels reduced in biofilm (51 out of 56) and planktonic culture (59 out of 63) of the dual-species model. This observed reduction in protein production agreed with a proteomic study of *P. gingivalis*, where it was cultivated in three species community with *F. nucleatum* and *S. gordoni* [26]. The study authors suggested that the microbial community provided physiological support to *P. gingivalis* and, in this way, reduced its stress. Accordingly, a plausible explanation for these findings, which are in line with previous studies [18,20,26], is that the presence of *F. nucleatum* proteins creates a supportive environment for *P. gingivalis* growth.

5. Conclusion

Our study has showed how two oral bacteria interact with each other on the proteome level and how the *F. nucleatum* presence influences the levels of multiple *P. gingivalis* proteins both in biofilm and planktonic culture. The data support the notion that *P. gingivalis* adapts to the biofilm condition by increasing levels of certain proteins; however, the presence of *F. nucleatum* mitigates this need by providing favourable growth conditions (Fig. 4).

The reported findings were obtained under *in vitro* laboratory setting and therefore should be interpreted with caution. Results of this study should be further validated under *in vivo* conditions, for example, in co-culture models of bacterial biofilm and oral epithelial cells [62] that have been applied to study the complexity of an oral microenvironment. The cellular response of *P. gingivalis* will likely change when it is associated with multispecies bacterial biofilm compared to a dual-species model. Proteomic studies of multispecies biofilms are an important area for future investigations, and in combination with gingival cell culture models, such studies will provide important insights into the biofilm formation and, consequently, for the prevention of periodontal diseases.

Availability of data

Data are available via http://www.proteomexchange.org/with identifier PXD008288.

Funding

This work was funded by grants from the Research Council of Norway and Gades Legat.

Authors' contributions

Study design (MMAM, VB, AHN, HGW), Funding (MMAM, VB), Experimental procedures (MMAM), Data analysis and interpretation (MMAM, VKP), Manuscript draft (MMAM, VKP), Text critical review (MMAM, VKP, AHN, HGW, VB).

Declaration of competing interest

The study funding sources are listed in the Acknowledgements. The authors have no financial/commercial conflicts of interest.

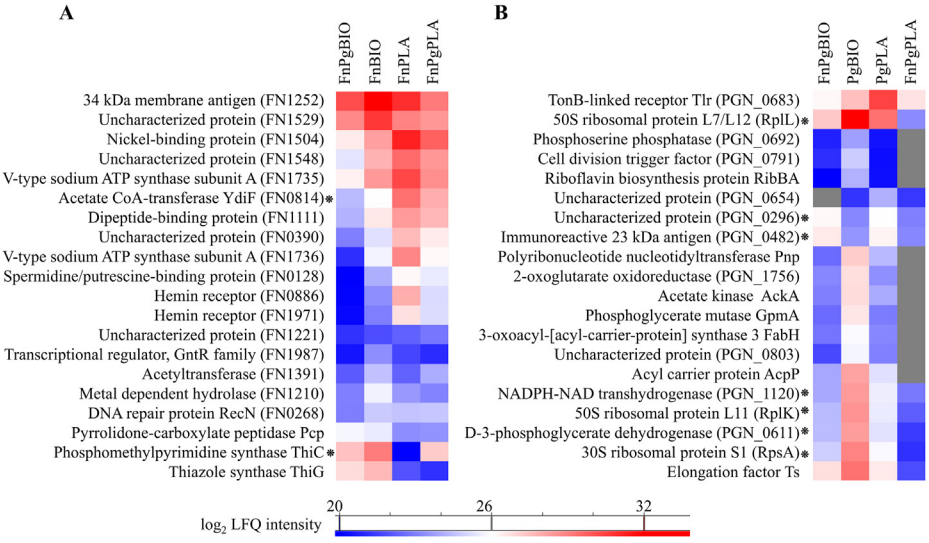

Fig. 3. Hierarchical clustering of 20 selected **A)** *F. nucleatum* and **B)** *P. gingivalis* proteins with differential expression across the biofilm and planktonic modes of growth and the single and dual-species models. Proteins with significantly different levels (p-value <0.05, $\log_2$ LFQ intensity >2) in at least two conditions are indicated by a star. Abbreviations: Fn - *F. nucleatum*, Pg - *P. gingivalis*, PLA – planktonic culture, BIO – biofilm. Means of 3 biological replicates are shown, and grey fields indicate missing values, *i.e.*, the protein was not detected, or its amounts were below quantifiable levels.

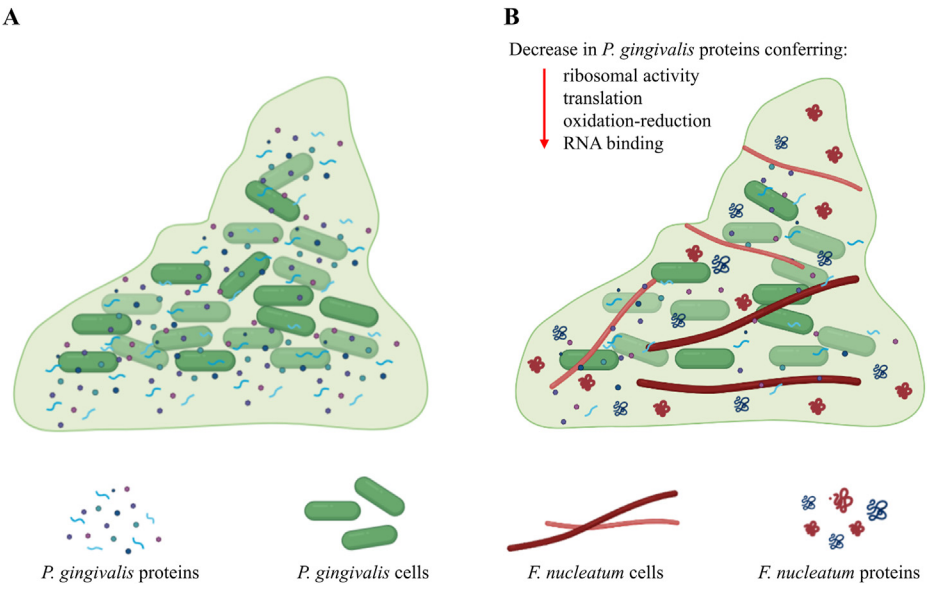

Fig. 4. Illustrations of *P. gingivalis* biofilm and its dual-species model with *F. nucleatum*. **A)** Single species biofilm model of *P. gingivalis* with highlighted bacterial cells and proteins. Compared to planktonic culture, *P. gingivalis* seems to adapt to the biofilm condition by increasing levels of certain proteins. **B)** In the dual-species model, the presence of *F. nucleatum* mitigates this need by providing favourable growth conditions for *P. gingivalis*. Functional categories of *P. gingivalis* proteins that were detected as significantly decreased in the dual-species biofilm, compared to *P. gingivalis* biofilm alone, are indicated. In both A and B, bacterial cells and proteins are not drawn to scale.

Acknowledgments

We acknowledge the Proteomic Unit at the University of Bergen, particularly Olav Mjaavatten, for the LC-MS/MS experiments support.

Appendix A. Supplementary data

Supplementary data to this article can be found online at https://doi.org/10.1016/j.anaerobe.2021.102449.

References

[1] S.S. Socransky, A.D. Haffajee, M.A. Cugini, C. Smith, R.L. Kent Jr., Microbial complexes in subgingival plaque, J. Clin. Periodontol. 25 (2) (1998) 134–144.
[2] C. Schaudinn, A. Gorur, D. Keller, P.P. Sedghizadeh, J.W. Costerton, Periodontitis: an archetypical biofilm disease, J. Am. Dent. Assoc. 140 (8) (2009) 978–986.
[3] B.L. Pihlstrom, B.S. Michalowicz, N.W. Johnson, Periodontal diseases, Lancet 366 (9499) (2005) 1809–1820.
[4] F. Carrouel, S. Viennot, J. Santamaria, P. Veber, D. Bourgeois, Quantitative molecular detection of 19 major pathogens in the interdental biofilm of periodontally healthy young adults, Front. Microbiol. 7 (2016) 840.
[5] P.E. Kolenbrander, Oral microbial communities: biofilms, interactions, and genetic systems, Annu. Rev. Microbiol. 54 (2000) 413–437.
[6] H.R. Lee, H.K. Jun, H.D. Kim, S.H. Lee, B.K. Choi, *Fusobacterium nucleatum* GroEL induces risk factors of atherosclerosis in human microvascular endothelial cells and ApoE(-/-) mice, Mol Oral Microbiol 27 (2) (2012) 109–123.
[7] C.W. Kaplan, X. Ma, A. Paranjpe, A. Jewett, R. Lux, S. Kinder-Haake, et al., *Fusobacterium nucleatum* outer membrane proteins Fap2 and RadD induce cell death in human lymphocytes, Infect. Immun. 78 (11) (2010) 4773–4778.
[8] M.R. Rubinstein, X. Wang, W. Liu, Y. Hao, G. Cai, Y.W. Han, *Fusobacterium nucleatum* promotes colorectal carcinogenesis by modulating E-cadherin/beta-catenin signaling via its FadA adhesin, Cell Host Microbe 14 (2) (2013) 195–206.
[9] A. Kumar, P.L. Thotakura, B.K. Tiwary, R. Krishna, Target identification in *Fusobacterium nucleatum* by subtractive genomics approach and enrichment analysis of host-pathogen protein-protein interactions, BMC Microbiol. 16 (2016) 84.
[10] V. Kapatral, I. Anderson, N. Ivanova, G. Reznik, T. Los, A. Lykidis, et al., Genome sequence and analysis of the oral bacterium *Fusobacterium nucleatum* strain ATCC 25586, J. Bacteriol. 184 (7) (2002) 2005–2018.
[11] V. Bakken, S. Aaro, T. Hofstad, E.N. Vasstrand, Outer membrane proteins as major antigens of *Fusobacterium nucleatum*, FEMS Microbiol. Immunol. 1 (8–9) (1989) 473–483.
[12] S.C. Holt, J.L. Ebersole, *Porphyromonas gingivalis, Treponema denticola,* and *Tannerella forsythia*: the "red complex", a prototype polybacterial pathogenic consortium in periodontitis, Periodontol. 2000 38 (2005) 72–122.
[13] R.J. Lamont, H.F. Jenkinson, Life below the gum line: pathogenic mechanisms of *Porphyromonas gingivalis*, Microbiol. Mol. Biol. Rev. 62 (4) (1998) 1244–1263.
[14] M. Naito, H. Hirakawa, A. Yamashita, N. Ohara, M. Shoji, H. Yukitake, et al., Determination of the genome sequence of *Porphyromonas gingivalis* strain ATCC 33277 and genomic comparison with strain W83 revealed extensive genome rearrangements in P. gingivalis, DNA Res. 15 (4) (2008) 215–225.
[15] J. Mysak, S. Podzimek, P. Sommerova, Y. Lyuya-Mi, J. Bartova, T. Janatova, et al., *Porphyromonas gingivalis:* major periodontopathic pathogen overview, J Immunol Res. 2014 (2014) 476068.
[16] L. Jia, N. Han, J. Du, L. Guo, Z. Luo, Y. Liu, Pathogenesis of important virulence factors of *Porphyromonas gingivalis* via toll-like receptors, Front Cell Infect Microbiol 9 (2019) 262.
[17] S. Periasamy, P.E. Kolenbrander, Mutualistic biofilm communities develop with *Porphyromonas gingivalis* and initial, early, and late colonizers of enamel, J. Bacteriol. 191 (22) (2009) 6804–6811.
[18] Z. Metzger, Y.Y. Lin, F. Dimeo, W.W. Ambrose, M. Trope, R.R. Arnold, Synergistic pathogenicity of *Porphyromonas gingivalis* and *Fusobacterium nucleatum* in the mouse subcutaneous chamber model, J. Endod. 35 (1) (2009) 86–94.
[19] M.M. Ali Mohammed, A.H. Nerland, M. Al-Haroni, V. Bakken, Characterization of extracellular polymeric matrix, and treatment of *Fusobacterium nucleatum* and *Porphyromonas gingivalis* biofilms with DNase I and proteinase K, J. Oral Microbiol. 5 (2013), https://doi.org/10.3402/jom.v5i0.20015.
[20] P.I. Diaz, P.S. Zilm, A.H. Rogers, *Fusobacterium nucleatum* supports the growth of *Porphyromonas gingivalis* in oxygenated and carbon-dioxide-depleted environments, Microbiology 148 (Pt 2) (2002) 467–472.
[21] D.J. Bradshaw, P.D. Marsh, G.K. Watson, C. Allison, Role of *Fusobacterium nucleatum* and coaggregation in anaerobe survival in planktonic and biofilm oral microbial communities during aeration, Infect. Immun. 66 (10) (1998) 4729–4732.
[22] Y. Saito, R. Fujii, K.I. Nakagawa, H.K. Kuramitsu, K. Okuda, K. Ishihara, Stimulation of *Fusobacterium nucleatum* biofilm formation by *Porphyromonas gingivalis*, Oral Microbiol. Immunol. 23 (1) (2008) 1–6.
[23] D. Polak, A. Wilensky, L. Shapira, A. Halabi, D. Goldstein, E.I. Weiss, et al., Mouse model of experimental periodontitis induced by *Porphyromonas gingivalis/Fusobacterium nucleatum* infection: bone loss and host response, J. Clin. Periodontol. 36 (5) (2009) 406–410.
[24] E.L. Hendrickson, T. Wang, D.A. Beck, B.C. Dickinson, C.J. Wright, J.L. R, et al., Proteomics of *Fusobacterium nucleatum* within a model developing oral microbial community, Microbiologyopen 3 (5) (2014) 729–751.
[25] Z. Zainal-Abidin, P.D. Veith, S.G. Dashper, Y. Zhu, D.V. Catmull, Y.Y. Chen, et al., Differential proteomic analysis of a polymicrobial biofilm, J. Proteome Res. 11 (9) (2012) 4449–4464.
[26] M. Kuboniwa, E.L. Hendrickson, Q. Xia, T. Wang, H. Xie, M. Hackett, et al., Proteomics of *Porphyromonas gingivalis* within a model oral microbial community, BMC Microbiol. 9 (2009) 98.
[27] R. Huang, M. Li, R.L. Gregory, Bacterial interactions in dental biofilm, Virulence 2 (5) (2011) 435–444.

[28] K. Sauer, A.K. Camper, G.D. Ehrlich, J.W. Costerton, D.G. Davies, *Pseudomonas aeruginosa* displays multiple phenotypes during development as a biofilm, J. Bacteriol. 184 (4) (2002) 1140–1154.
[29] J.W. Costerton, Introduction to biofilm, Int. J. Antimicrob. Agents 11 (3–4) (1999) 217–221, discussion 37-9.
[30] A. Llama-Palacios, O. Potupa, M.C. Sanchez, E. Figuero, D. Herrera, M. Sanz, Proteomic analysis of *Fusobacterium nucleatum* growth in biofilm versus planktonic state, Mol Oral Microbiol 35 (4) (2020) 168–180.
[31] K. Maeda, H. Nagata, M. Ojima, A. Amano, Proteomic and transcriptional analysis of interaction between oral microbiota *Porphyromonas gingivalis* and *Streptococcus oralis*, J. Proteome Res. 14 (1) (2015) 82–94.
[32] C.-S. Ang, P.D. Veith, S.G. Dashper, E.C. Reynolds, Application of 16O/18O reverse proteolytic labeling to determine the effect of biofilm culture on the cell envelope proteome of *Porphyromonas gingivalis* W50, Proteomics 8 (8) (2008) 1645–1660.
[33] M.M. Mohammed, V.K. Pettersen, A.H. Nerland, H.G. Wiker, V. Bakken, Quantitative proteomic analysis of extracellular matrix extracted from mono- and dual-species biofilms of *Fusobacterium nucleatum* and *Porphyromonas gingivalis*, Anaerobe 44 (2017) 133–142.
[34] V.K. Pettersen, H. Steinsland, H.G. Wiker, Distinct metabolic features of pathogenic *Escherichia coli* and *Shigella* spp. determined by label-free quantitative proteomics, Proteomics 21 (2) (2021) 2000072.
[35] J. Clifton, F. Huang, M. Rucevic, L. Cao, D. Hixson, D. Josic, Protease inhibitors as possible pitfalls in proteomic analyses of complex biological samples, J Proteomics 74 (7) (2011) 935–941.
[36] J.R. Wisniewski, A. Zougman, N. Nagaraj, M. Mann, Universal sample preparation method for proteome analysis, Nat. Methods 6 (5) (2009) 359–362.
[37] J. Rappsilber, M. Mann, Y. Ishihama, Protocol for micro-purification, enrichment, pre-fractionation and storage of peptides for proteomics using StageTips, Nat. Protoc. 2 (8) (2007) 1896–1906.
[38] J. Cox, M. Mann, MaxQuant enables high peptide identification rates, individualized p.p.b.-range mass accuracies and proteome-wide protein quantification, Nat. Biotechnol. 26 (12) (2008) 1367–1372.
[39] J. Herschend, Z.B.V. Damholt, A.M. Marquard, B. Svensson, S.J. Sørensen, P. Hägglund, et al., A meta-proteomics approach to study the interspecies interactions affecting microbial biofilm development in a model community, Sci. Rep. 7 (1) (2017) 16483.
[40] J. Cox, M.Y. Hein, C.A. Luber, I. Paron, N. Nagaraj, M. Mann, Accurate proteome-wide label-free quantification by delayed normalization and maximal peptide ratio extraction, termed MaxLFQ, Mol. Cell. Proteomics 13 (9) (2014) 2513–2526.
[41] S. Tyanova, T. Temu, P. Sinitcyn, A. Carlson, M.Y. Hein, T. Geiger, et al., The Perseus computational platform for comprehensive analysis of (prote)omics data, Nat. Methods 13 (9) (2016) 731–740.
[42] da W. Huang, B.T. Sherman, R.A. Lempicki, Systematic and integrative analysis of large gene lists using DAVID bioinformatics resources, Nat. Protoc. 4 (1) (2009) 44–57.
[43] D. Binns, E. Dimmer, R. Huntley, D. Barrell, C. O'Donovan, R. Apweiler, QuickGO: a web-based tool for Gene Ontology searching, Bioinformatics 25 (22) (2009) 3045–3046.
[44] K. Imai, N. Asakawa, T. Tsuji, F. Akazawa, A. Ino, M. Sonoyama, et al., SOSUI-GramN: high performance prediction for sub-cellular localization of proteins in gram-negative bacteria, Bioinformation 2 (9) (2008) 417–421.
[45] E.W. Deutsch, A. Csordas, Z. Sun, A. Jarnuczak, Y. Perez-Riverol, T. Ternent, et al., The ProteomeXchange consortium in 2017: supporting the cultural change in proteomics public data deposition, Nucleic Acids Res. 45 (D1) (2017) D1100–D1106.
[46] K.W. Bayles, The biological role of death and lysis in biofilm development, Nat. Rev. Microbiol. 5 (9) (2007) 721–726.
[47] S.E. Gharbia, H.N. Shah, Characteristics of glutamate dehydrogenase, a new diagnostic marker for the genus *Fusobacterium*, J. Gen. Microbiol. 134 (2) (1988) 327–332.
[48] D.N. Toussi, X. Liu, P. Massari, The FomA porin from *Fusobacterium nucleatum* is a Toll-like receptor 2 agonist with immune adjuvant activity, Clin. Vaccine Immunol. 19 (7) (2012) 1093–1101.
[49] C. Zenobia, G. Hajishengallis, *Porphyromonas gingivalis* virulence factors involved in subversion of leukocytes and microbial dysbiosis, Virulence 6 (3) (2015) 236–243.
[50] P. Romero-Lastra, M.C. Sanchez, H. Ribeiro-Vidal, A. Llama-Palacios, E. Figuero, D. Herrera, et al., Comparative gene expression analysis of *Porphyromonas gingivalis* ATCC 33277 in planktonic and biofilms states, PLoS One 12 (4) (2017), e0174669.
[51] S. Rajamani, W.D. Bauer, J.B. Robinson, J.M. Farrow 3rd, E.C. Pesci, M. Teplitski, et al., The vitamin riboflavin and its derivative lumichrome activate the LasR bacterial quorum-sensing receptor, Mol. Plant Microbe Interact. 21 (9) (2008) 1184–1192.
[52] E. Marsili, D.B. Baron, I.D. Shikhare, D. Coursolle, J.A. Gralnick, D.R. Bond, *Shewanella secretes* flavins that mediate extracellular electron transfer, Proc. Natl. Acad. Sci. U. S. A. 105 (10) (2008) 3968–3973.
[53] Q. Xia, T. Wang, F. Taub, Y. Park, C.A. Capestany, R.J. Lamont, et al., Quantitative proteomics of intracellular *Porphyromonas gingivalis*, Proteomics 7 (23) (2007) 4323–4337.
[54] M.A. Pysz, S.B. Conners, C.I. Montero, K.R. Shockley, M.R. Johnson, D.E. Ward, et al., Transcriptional analysis of biofilm formation processes in the anaerobic, hyperthermophilic bacterium *Thermotoga maritima*, Appl. Environ. Microbiol. 70 (10) (2004) 6098–6112.
[55] Y. Fardini, X. Wang, S. Temoin, S. Nithianantham, D. Lee, M. Shoham, et al., *Fusobacterium nucleatum* adhesin FadA binds vascular endothelial cadherin and alters endothelial integrity, Mol. Microbiol. 82 (6) (2011) 1468–1480.
[56] Y.-J. Jung, H.-K. Jun, B.-K. Choi, *Porphyromonas gingivalis* suppresses invasion of *Fusobacterium nucleatum* into gingival epithelial cells, J. Oral Microbiol. 9 (1) (2017) 1320193.
[57] J. Katz, Q.B. Yang, P. Zhang, J. Potempa, J. Travis, S.M. Michalek, et al., Hydrolysis of epithelial junctional proteins by *Porphyromonas gingivalis* gingipains, Infect. Immun. 70 (5) (2002) 2512–2518.
[58] P. Romero-Lastra, M.C. Sanchez, A. Llama-Palacios, E. Figuero, D. Herrera, M. Sanz, Gene expression of *Porphyromonas gingivalis* ATCC 33277 when growing in an in vitro multispecies biofilm, PLoS One 14 (8) (2019), e0221234.
[59] P.D. Veith, D.G. Gorasia, E.C. Reynolds, Towards defining the outer membrane proteome of *Porphyromonas gingivalis*, Mol Oral Microbiol 36 (1) (2021) 25–36.
[60] J.C. Scott, B.A. Klein, A. Duran-Pinedo, L. Hu, M.J. Duncan, A two-component system regulates hemin acquisition in *Porphyromonas gingivalis*, PLoS One 8 (9) (2013) e73351-e.
[61] N. Scheres, R.J. Lamont, W. Crielaard, B.P. Krom, LuxS signaling in *Porphyromonas gingivalis*-host interactions, Anaerobe 35 (2015) 3–9.
[62] S.E. Mountcastle, S.C. Cox, R.L. Sammons, S. Jabbari, R.M. Shelton, S.A. Kuehne, A review of co-culture models to study the oral microenvironment and disease, J. Oral Microbiol. 12 (1) (2020) 1773122.